THE UNIVERSITY *of* EDINBURGH



# Tensile strengths of flocculated compacted unsaturated soils

**Citation for published version:**
Beckett, CTS, Smith, JC, Ciancio, D & Augarde, CE 2015, 'Tensile strengths of flocculated compacted unsaturated soils' Geotechnique Letters, vol. 5, no. 4, pp. 254-260. DOI: 10.1680/jgele.15.00087

**Digital Object Identifier (DOI):**
10.1680/jgele.15.00087



**Published In:**
Geotechnique Letters

# Tensile strengths of flocculated compacted unsaturated soils

C.T.S. Beckett[a,], J.C. Smith[b], D. Ciancio[a], C.E. Augarde[b]

[a]*School of Civil, Environmental and Mining Engineering, University of Western Australia, Perth, WA 6009*
[b]*School of Engineering and Computing Sciences, Durham University, Durham, DH1 3LE, UK*

---

**Abstract**

Flocculating agents can be introduced to soils through a number of natural or anthropogenic processes. This paper investigates the effect of flocculant addition (aqueous $CaCl_2$) on the tensile strengths of two soils of differing flocculation susceptibility. Tensile strengths were found using the Brazilian (direct splitting) test for a range of suction values. A decrease in tensile strength was found for a soil with a high clay content, which was consistent with previous literature findings. However, the strength of the lower clay-content soil unexpectedly increased. Results were interpreted using the Extended Mohr Coulomb (EMC) Yield Criterion comprising two planar yield surfaces, fitted to data above and below the residual suction value. Changes in EMC parameters were used to infer changes in material behaviour on $CaCl_2$ addition. Results have important implications for the design of geotechnical structures, for example engineered cover systems, exposed to flocculating conditions.

*Keywords:* Flocculation, tensile strength, Brazilian test, suction

---

*Email addresses:* `christopher.beckett@uwa.edu.au` (C.T.S. Beckett), `j.c.smith@dur.ac.uk` (J.C. Smith), `daniela.ciancio@uwa.edu.au` (D. Ciancio), `charles.augarde@dur.ac.uk` (C.E. Augarde)

## 1. Introduction

Many processes introduce flocculating agents to soils. For example, they are widely used in the mining industry to improve tailings dewatering, consolidation times and transportability (Williams and Jones, 2005). Closure and rehabilitation of tailings storage sites typically involves the placement of unsaturated soil cover layers in direct contact with this treated material. How flocculants effect unsaturated soil properties must therefore be understood; for example, unexpected cracking can lead to increased water infiltration or decomposition gas emission. Root penetration resistance may also be affected, with beneficial or problematic implications depending on the cover's function.

## 2. Soil flocculation

Flocculating agents modify the behaviour of soil clay particles by modifying cation adsorption and surface charge. The *lyotropic series* gives the order of the strength of bonding to the cation exchange surface (i.e. cation exchange preference):

$$Al^{3+} > Ca^{2+} > Mg^{2+} > NH^{4+} > K^{+} > Na^{+} \quad (1)$$

Flocculants lie to the left of (1), dispersants to the right (Grant et al., 1992). Previous investigations have indicated that tensile strengths of clayey soils are improved through the addition of dispersants (Dexter and Chan, 1991; Rycroft et al., 2002; Sou/Dakouré et al., 2013; Deng et al., 2014), but reduced through flocculation (Barzegar et al., 1994a,b, 1996; Dontsova and Norton, 2002). Critically, however, these works comprised several shortfalls:

- soil microstructure was not considered during sample preparation: material was either in a field condition or reconstituted, with no record of dry density;

- testing was conducted on aggregate-scale specimens (≤12mm), which do not represent bulk soil properties;
- soil suction was generally not considered: results may have been affected by poor suction equilibration or hysteresis.

This paper addresses some of these issues. Here, the splitting tensile ("Brazilian") test is used to investigate the effect of flocculant addition on the tensile strength of specimens of two engineered soils equilibrated to a wide range of suction conditions. Results are interpreted according to Extended Mohr-Coulomb theory, in order to identify changes in unsaturated material properties responsible for the observed behaviour.

## 3. Experimental procedure

### *3.1. Materials*

'Engineered' soils were used for this investigation in preference to natural soils to improve material grading and particle mineralogy control. Two soils were formed by combining *a priori* known quantities of silty-clay ("Birtley clay", LL 58.8%, PL 25.7%, 50% kaolinitic clay by mass (Smith and Augarde, 2014)), sand and gravel, sieved to remove particles larger than 10mm. Soil constituents (by mass) are given in Table 1 and particle grading curves are shown in Figure 1. As flocculants interact with the soil clay particles, engineered soils were designed to investigate the effect of changing clay contents on strength change on $CaCl_2$ addition. A low gravel content was used to improve specimen compaction and testing (Beckett, 2011). Soils are labelled according to their silty-clay:sand:gravel content ratios by mass, where $[x]$ in Table 1 gives the maximum percentage deviation between designed and actual mix proportions (Hall and Djerbib, 2004; Smith

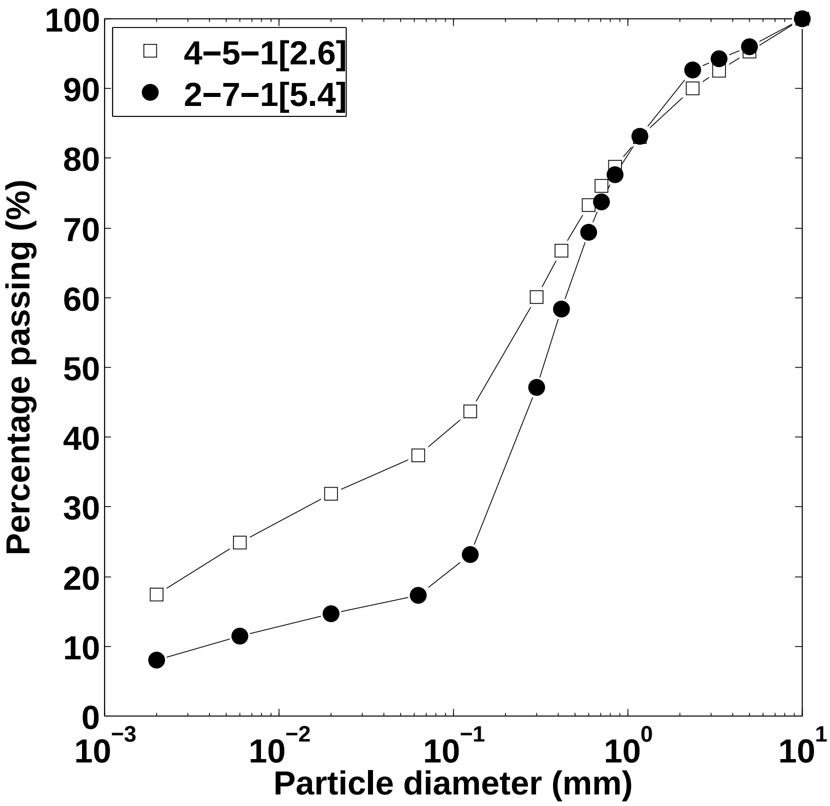


Figure 1: Particle grading curves for Soils 4-5-1 and 2-7-1 (untreated)

and Augarde, 2013). *Untreated* material optimum water contents (OWCs) and maximum dry densities ($\rho_{d_{max}}$), determined using the Light Proctor compaction test (BS 1377:1990), are also given in Table 1.

(Insert Figure 1 somewhere near here)

(Insert Table 1 somewhere near here)

Table 1: Soil constituents, OWC and $\rho_{d_{max}}$

| Soil | Silty-clay (%) | Sand (%) | Gravel (%) | OWC (%) | $\rho_{d_{max}}$ (kg/m$^3$) |
|---|---|---|---|---|---|
| 4-5-1[2.6] | 40 | 50 | 10 | 11.0 | 1940 |
| 2-7-1[5.4] | 20 | 70 | 10 | 12.0 | 1960 |

### *3.2. Tensile test specimen manufacture*

Tensile strength was selected to compare treated and untreated material behaviour due to the concern of cracking in engineered cover systems. Specimens were tested using the Brazilian test; it is envisaged that its low cost and convenience would make it ideal for cover material bulk testing. Although originally developed for hard materials, for example rocks, the Brazilian test is also capable of testing low-plasticity soils and specimens comprising multiple compaction planes (Frydman, 1964; Dexter and Kroesbergen, 1985). Direct testing methods (e.g. Lu et al. (2007)) were not deemed suitable due to the high anticipated soil strengths.

#### *3.2.1. Specimen size*

Specimen size greatly affects the tensile strength inferred from the Brazilian test, due to the relative size of the loaded surface (Rocco et al., 1999). Specimens of different diameters were manufactured to investigate size effect on measured tensile strength. Untreated ∅50mm and ∅100mm (2:1 diameter-to-length ratio) Soil 4-5-1 and 2-7-1 specimens were compacted to $\rho_{d_{max}}$ given in Table 1, at the material OWC. Six specimens were tested per soil and specimen size. Specimens were air-dried to water contents of 4.0±0.1% and wrapped in clear plastic for 48 hours for suction equilibration. 4.0% was selected as it produced sufficient strength for transportation in a relatively short drying time. Specimens were then tested to failure at a constant displacement rate of 0.2mm/min, suggested

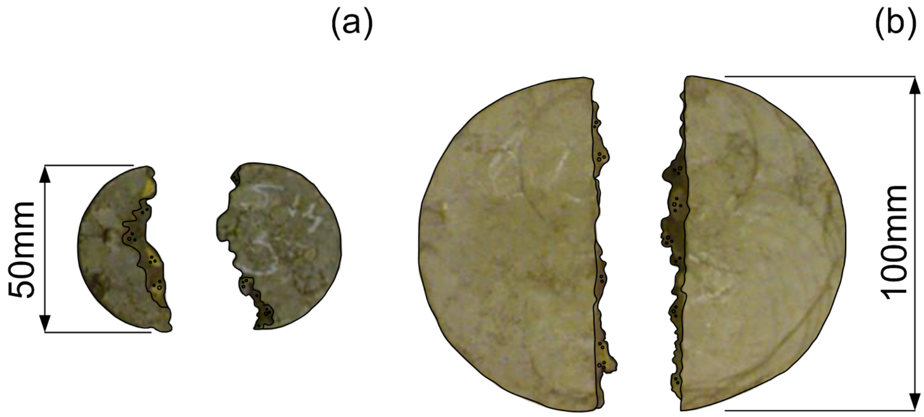


Figure 2: Failure of Brazilian test samples indicating non-vertical and vertical failure cracks: a) 50 mm diameter 25 mm high; b) 100 mm diameter 50 mm high. Outlines and shading added for clarity.

by Stirling et al. (2015) to be sufficiently slow for repeatable tensile strength testing. Tensile strength ($\sigma_t$) was determined via

$$\sigma_t = \frac{P}{\pi R L}, \tag{2}$$

where $P$ is the peak applied compressive load and $R$ and $L$ are the specimen radius and length respectively. For convenience, tensile strength has been taken as *positive.*

Significant variability was found for $\sigma_t$ for ∅50mm specimens, whilst good consistency was found for all ∅100mm specimens (Table 2). Typical failure cracks for these specimens are shown in Figure 2. Higher ∅50mm variability was due to the greater influence of larger soil particles on crack formation and propagation (Eqn 2 assumes a planar failure crack). ∅100mm specimens were therefore used for further testing.

(Insert Figure 2 somewhere near here)

Table 2: Average tensile strength and standard deviation for different specimen diameters. $s$: standard deviation; CV: coefficient of variation.

| Soil | Diameter (mm) | $\sigma_t$ (kPa) | $s$ (kPa, CV (%)) |
|---|---|---|---|
| 4-5-1 | 50 | 59.1 | 5.6, 9.5 |
| 4-5-1 | 100 | 86.4 | 4.7, 5.4 |
| 2-7-1 | 50 | 50.2 | 8.5, 16.9 |
| 2-7-1 | 100 | 63.8 | 2.7, 4.2 |

(Insert Table 2 somewhere near here)

### *3.2.2. Flocculated specimens*

Calcium chloride ($CaCl_2$) was used as a flocculating agent due to its ready availability and non-toxic nature. It is noted, however, that it is unlikely that pure $CaCl_2$ would be purposefully added to soil as a source of calcium, given its expense and the availability of cheaper sources, for example gypsum.

∅100mm specimens of soils 4-5-1 and 2-7-1 were manufactured using either deionised water or a solution of 40dS/m $CaCl_2$ (3.1% $CaCl_2$ content by water mass). 40dS/m was selected to be representative of saline groundwater concentrations (Clayton et al., 1995). Wetted soil was left in a sealed bag to equilibrate for 48 hours after wetting prior to manufacture. All specimens were compacted to the *untreated* soil $\rho_{d,max}$ (at the corresponding OWC) given in Table 1, using the previously-described procedure. Once compacted, specimens were transferred to wire racks and air-dried to the desired water content for testing, whereupon they were wrapped in clear plastic for 48 hours for suction equilibration (all specimens were therefore tested under drying conditions). Specimens were then removed from their wrapping and tested, using the Brazilian test, to failure at a constant displacement rate of 0.2mm/min. $\sigma_t$ was then determined via Eqn 2.

### 3.3. Retention property testing

Treated and untreated soil retention properties were determined through a combination of filter paper and vapour equilibrium (for suctions >10MPa) testing. These methods were selected in preference to direct suction measurement (e.g. tensiometers) as they were able to cover the large range of suctions anticipated. Filter paper testing was conducted as per ASTM D5298-10 . The relationship

$$\ln \psi_t = -4.6234 - 3.6454 \ln(w_{fp}) \tag{3}$$

was used to calculate total suction ($\psi_t$) values from suspended filter paper gravimetric water content, $w_{fp}$. Eqn 3 was determined via a best-fit solution to filter paper data presented in Hamblin (1981). Soil water retention curves (SWRCs) for Soils 4-5-1 and 2-7-1 are shown in Figures 3 and 4 respectively.

Total suction values were approximated using

$$S_r = \left(1 + \frac{\log\left(1 + \frac{\psi_t}{10^9}\right)}{\log(2)}\right) \times \frac{1}{\left(\ln\left(e + \left(\frac{\psi_t}{a}\right)^n\right)\right)^m} \tag{4}$$

where $S_r$ is the degree of saturation and $e$ is the Euler number ($\approx 2.7183$). Fitting parameter $a$, $m$ and $n$, residual suction ($\psi_{t,res}$) and saturation ($S_{r,res}$) values are given in Table 3 (Fredlund and Xing, 1994). Eqn 4 was used to determine specimen suction conditions at testing (i.e. after drying) from measured $S_r$ values.

Figures 3 and 4 show an increase in $\psi_t$ for given $S_r$ values; this is due to the addition of $CaCl_2$ and an increase in osmotic suction (Dao et al., 2008). The effect of the addition of the flocculant agent is evident through increased $S_{r,res}$ and $\psi_{t,res}$ values for both soils, which indicate a change in soil structure. Complementary information regarding soil structural changes, for example as obtained by

Table 3: Fitting parameters used with Eqn 4

| Soil | | $a$ | $m$ | $n$ | $\psi_{t,res}$ (MPa) | $S_{r,res}$ |
|---|---|---|---|---|---|---|
| 4-5-1 | 0 dS/m | 1.60 | 0.90 | 3.50 | 4.0 | 0.26 |
| | 40 dS/m | 2.10 | 0.60 | 2.50 | 10.0 | 0.33 |
| 2-7-1 | 0 dS/m | 1.00 | 0.85 | 4.75 | 2.2 | 0.22 |
| | 40 dS/m | 1.25 | 0.85 | 2.50 | 6.0 | 0.28 |

Scanning Electron Microscopy (SEM), X-Ray CT (XRCT) or Mercury Intrusion Porosimmetry (MIP) is, unfortunately, not available.

(Insert Figure 3 somewhere near here)

(Insert Figure 4 somewhere near here)

(Insert Table 3 somewhere near here)

## 4. Results and discussion

### *4.1. Tensile strengths*

Variations in $\sigma_t$ with changing $S_r$ are compared in Figures 5 and 6 for treated and untreated Soils 4-5-1 and 2-7-1 respectively. Linear relationships have been added to indicate the rough data trends. All specimens displayed nominally-linear failure cracks, as shown in Figure 2(b), indicating that the use of Eqn 2 is valid.

Figure 5 shows a general reduction in $\sigma_t$ on $CaCl_2$ treatment, which is typical of results for clayey soils found in previous investigations. However, the opposite is shown results in Figure 6: an unexpected *increase* in $\sigma_t$ is observed. Notably, $\sigma_t$ results and trend gradients are similar for both treated soils (Figure 7); additional data is, however, required to determine whether this similarity is significant.

(Insert Figure 5 somewhere near here)

(Insert Figure 6 somewhere near here)

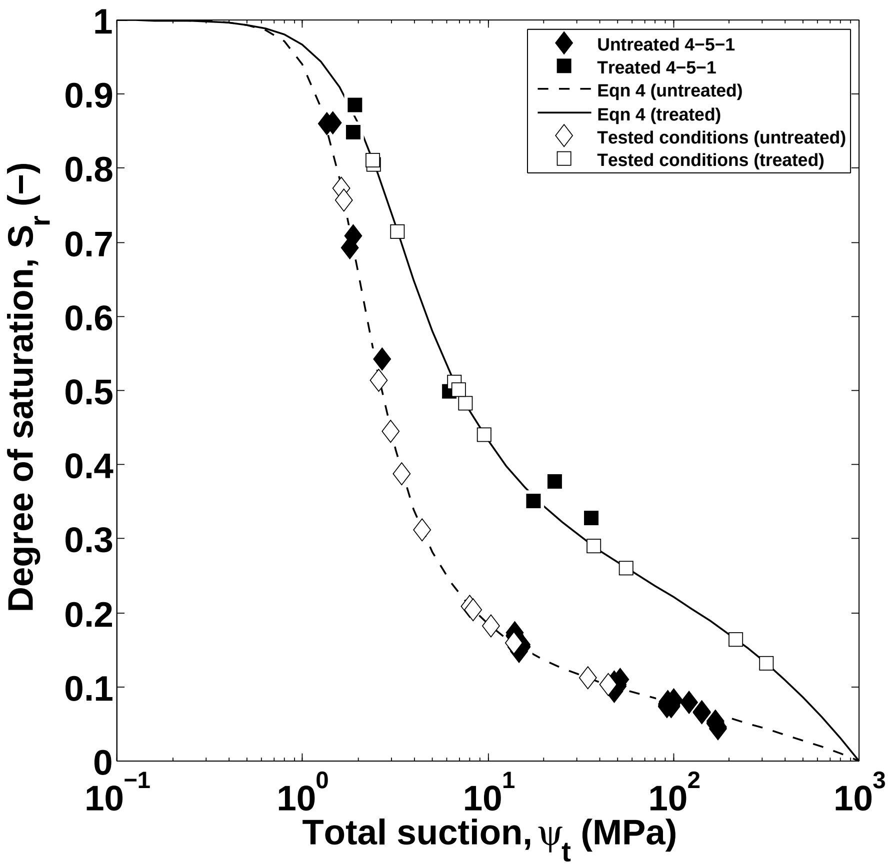


Figure 3: Treated and untreated SWRCs for soil 4-5-1. White markers show drying suction conditions for treated and untreated Brazilian test specimens.

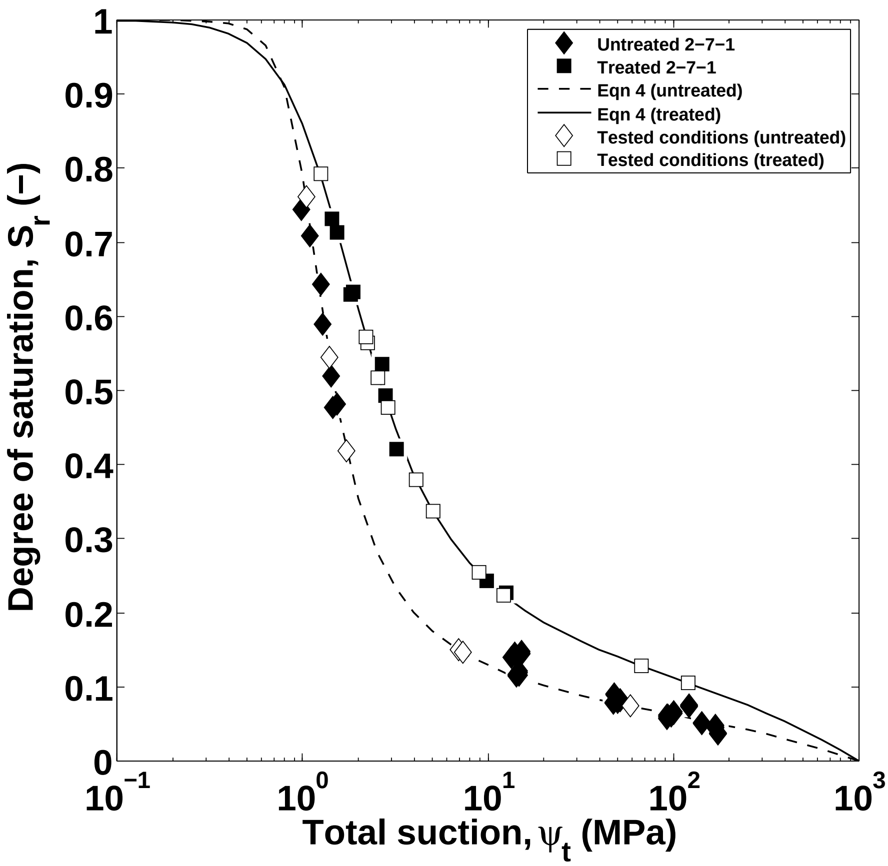


Figure 4: Treated and untreated SWRCs for soil 2-7-1. White markers show drying suction conditions for treated and untreated Brazilian test specimens.

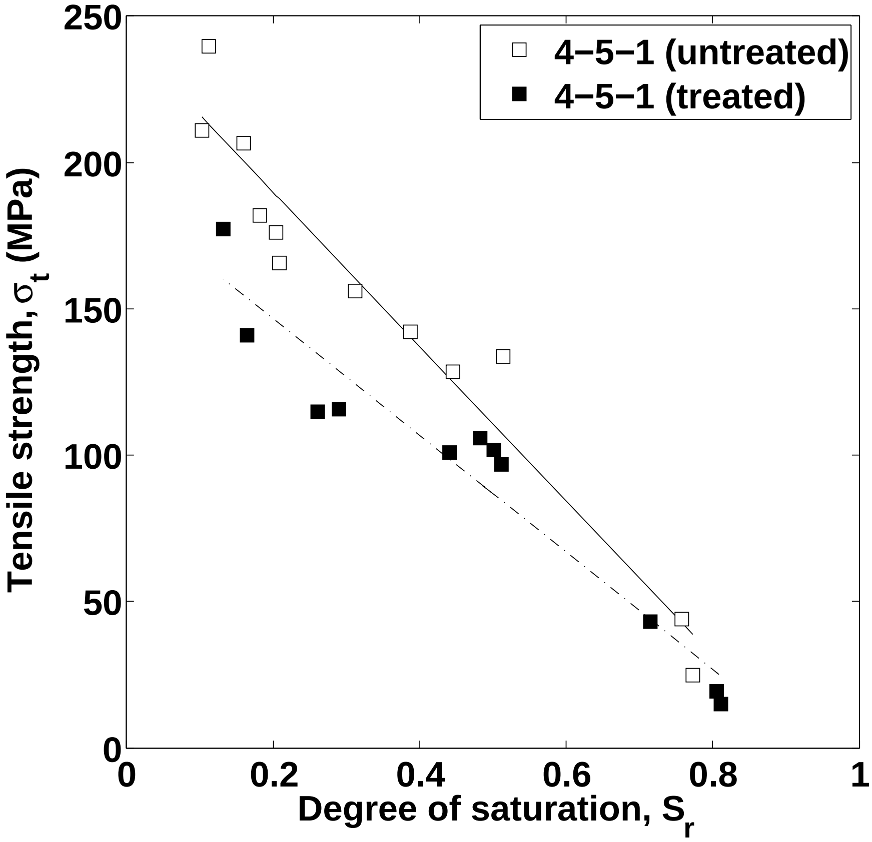


Figure 5: Tensile strength against degree of saturation for treated and untreated Soil 4-5-1 specimens

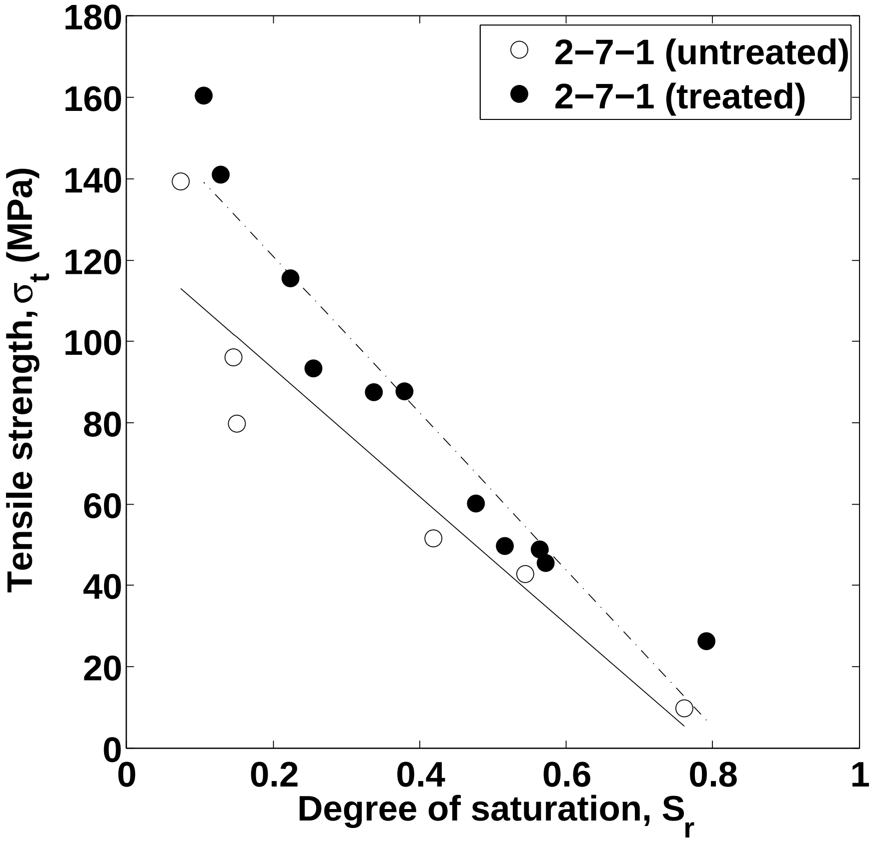


Figure 6: Tensile strength against degree of saturation for treated and untreated Soil 2-7-1 specimens

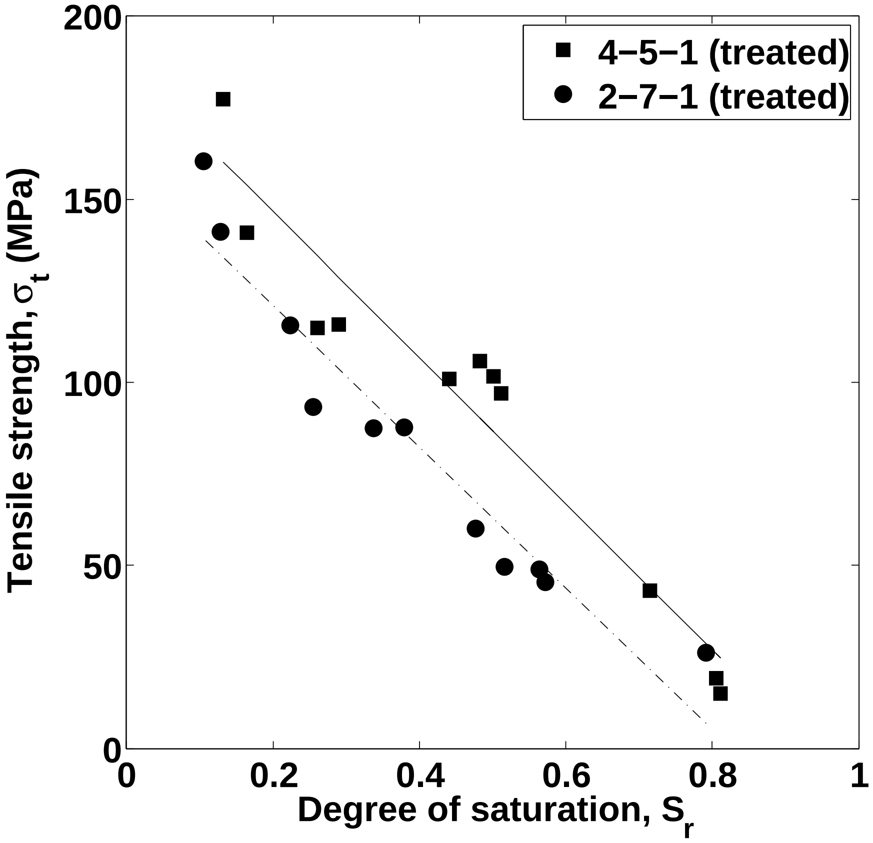


Figure 7: Comparison of treated Soil 4-5-1 and 2-7-1 results, with descriptive linear trends.

(Insert Figure 7 somewhere near here)

### *4.2. Extended Mohr-Coulomb analysis*

The Extended Mohr-Coulomb Yield Criterion (EMC) was used to interpret observed changes in $\sigma_t$ with associated changes in suction. The EMC approach adds a suction dimension to the familiar Mohr-Coulomb criterion. Shear strength, $\tau_f$, is given by:

$$\tau_f = c + (\sigma_f - u_a)\tan(\phi) + (\psi)\tan(\phi^b) \tag{5}$$

where $c$ is apparent cohesion, $\sigma_f$ is the normal stress corresponding to $\tau_f$, $u_a$ is pore air pressure (usually assumed to equal zero) and $\psi$ is suction. $\phi$ and $\phi^b$ are friction angles describing the change in $\tau_f$ with $\sigma$ (as for the saturated case) and $\tau_f$ with $\psi$ respectively (Fredlund et al., 1978). It is generally accepted that $\phi^b$ is a function of $S_r$ and diminishes to small values as $S_r$ approaches zero. Construction of the EMC failure envelope for a Brazilian test conducted at some non-zero suction value $\psi$ is shown in Figure 8 (Jaeger et al. (2007), reported in Consoli et al. (2014)). The relationships $\sigma_3 = \sigma_t$ and $\sigma_1 = -3\sigma_t$ are derived in Li and Wong (2013) and are valid provided $\dfrac{a}{y_1}$ is less than 0.27, where $a$ is the width of the deformed contact region and $y_1$ is the change in axial diameter (Frydman, 1964). These relationships are used here as little deformation ($\leq$1mm reduction in diameter, negligible flattening of contact area) occurred during testing.

(Insert Figure 8 somewhere near here)

Figure 9 shows calculated Mohr's circles for untreated Soil 4-5-1 specimens. A distinct change in the rate of circle growth with increasing $\psi_t$ is seen either side of $\psi_{t,res}$ (demarked in Figure 9). The residual suction can be considered to be the transition between continuous (funicular) and discontinuous (pendular) water phases (Schubert (1975), reported in Song et al. (2012)); it is therefore reasonable

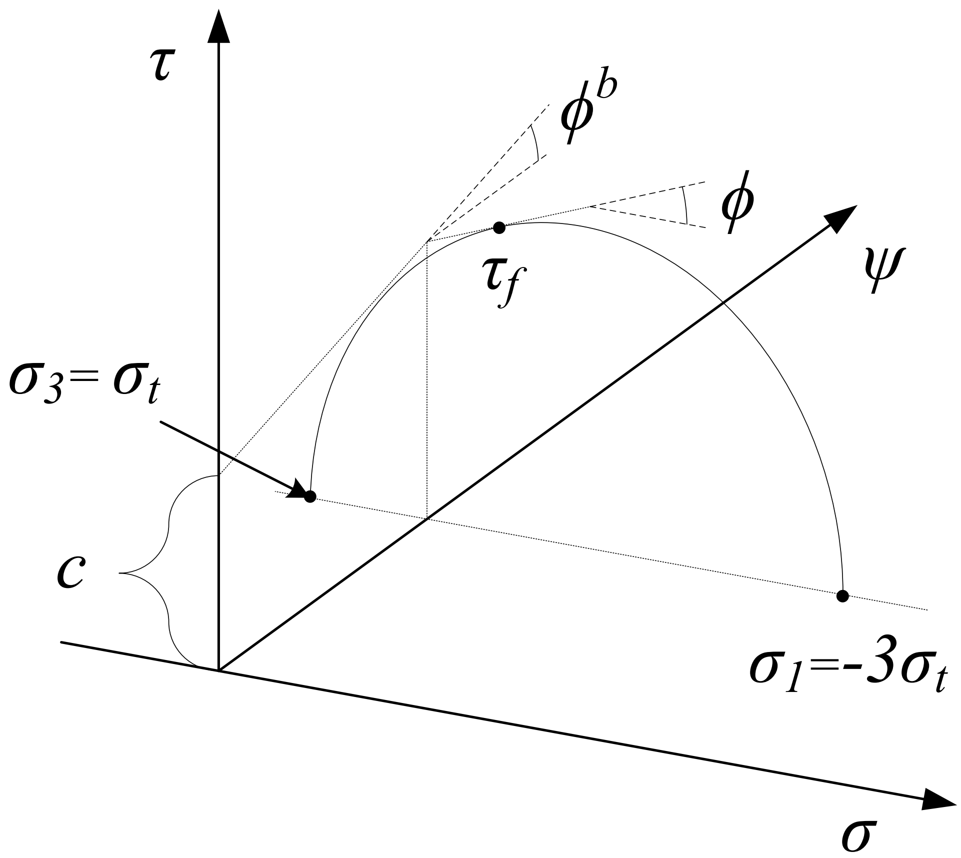


Figure 8: Example Brazilian test EMC failure surface construction

that a mechanistic change in the contribution of suction to strength occurs at this point. Fitting planes to data $< \psi_{t,res}$ produced negative $c$ values, which is not consistent with established EMC theory. A single plane was therefore fitted to data $\geq \psi_{t,res}$. Fredlund et al. (1996) showed that changes in $\phi^b$ are related to those in $\dfrac{dS_r}{d\psi}$; as $S_r$ changes little with $\psi_t$ in the residual suction range, a single plane is suitable to describe data in this region. The significance of negative $c$ values below $\psi_{t,res}$ is a topic for further study. Shear strengths predicted by the fitted failure plane, $\tau_{f,p}$, can be calculated via

$$\tau_{f,p} = c_{res} + (\sigma_f - u_a)\tan(\phi_{res}) + (\psi_t)\tan(\phi^b_{res}) \tag{6}$$

where subscript $res$ denotes parameters for suctions above $\psi_{t,res}$. $\sigma_f$ is found via $\sigma_f = \sigma_t(1 - 2\sin\phi)$, using the appropriate value of $\phi$ and where $\sigma_t$ is the measured value of tensile strength, found using Eqn 2. Predicted tensile strength ($\sigma_{t,p}$) can then be found via

$$\sigma_{t,p} = \text{centre} - \text{radius} = \sigma_f + \tau_{f,p}\left(\sin(\phi_{res}) - \frac{1}{\cos(\phi_{res})}\right) \tag{7}$$

using the appropriate value of $\tau_f$. Fitted EMC parameter and $r^2$ values are given in Table 4. Geometrical relationships used in the derivation of Eqn 7 are shown in Figure 10.

Measured against predicted values of $\sigma_t$ for all tested soil conditions are shown in Figure 11. That a good approximation to $\sigma_t$ was found in Figure 11 is to be expected, given the fitting nature of failure plane selection. However, the distinction between changes in $\sigma_t$ with $\psi_t$ above and below $\psi_{t,res}$ is readily apparent, supporting the interpretation of a mechanistic change in suction's contribution

Table 4: Fitted EMC failure surface parameter values

| Soil | Treatment | $c_{res}$ (kPa) | $\phi_{res}$ ($^\circ$) | $\phi^b_{res}$ ($^\circ$) | $r^2$ |
|---|---|---|---|---|---|
| 4-5-1 | 0 dS/m | 272.1 | 24.6 | 0.15 | 0.92 |
| | 40 dS/m | 173.3 | 23.1 | 0.02 | 0.94 |
| 2-7-1 | 0 dS/m | 134.6 | 23.6 | 0.10 | 0.98 |
| | 40 dS/m | 166.7 | 23.6 | 0.05 | 0.97 |

to strength between these two regions.

(Insert Figure 9 somewhere near here)

(Insert Figure 10 somewhere near here)

(Insert Figure 11 somewhere near here)

(Insert Table 4 somewhere near here)

Changes in EMC parameter values in Table 4 can explain observed changes in $\sigma_t$ with $S_r$ on $CaCl_2$ addition in Figures 5 and 6. The effect of flocculant addition on EMC parameters was mostly consistent between soils:

- $\phi^b_{res}$ decreased (more severely for Soil 4-5-1);
- little change $\phi_{res}$ occurred.

However, $c_{res}$ decreased for Soil 4-5-1 but increased for Soil 2-7-1. A decrease in $c_{res}$ demonstrates a reduced contribution to strength for suctions $> \psi_{t,res}$. Contrariwise, this contribution increased for Soil 2-7-1. These effects combined to produce the unexpected increase in $\sigma_t$ for Soil 2-7-1 on $CaCl_2$ addition, but the traditional decrease in $\sigma_t$ for Soil 4-5-1, suggestibly due to its higher flocculation susceptibility. This observation has important implications for geotechnical structures: if soils are only marginally susceptible to flocculation, an increase in tensile strength may occur instead of an anticipated decrease which may, for example, prevent root penetration.

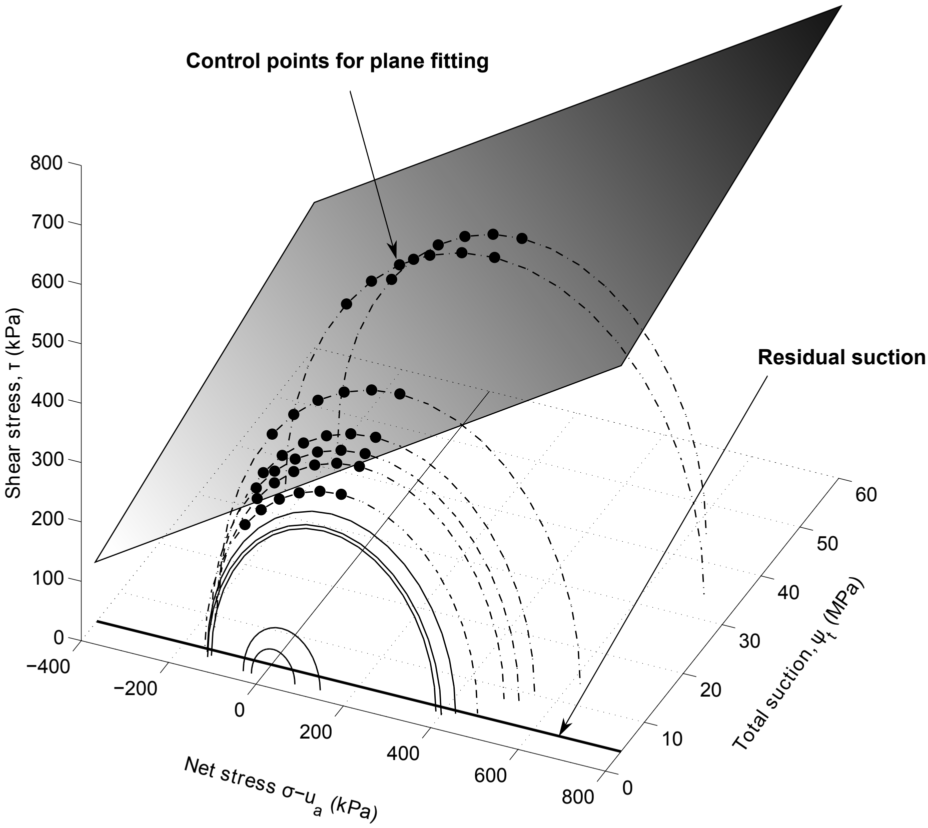


Figure 9: EMC failure surface for untreated Soil 4-5-1 above $\psi_{t,res}$. Solid lines (–): Mohr's circles below $\psi_{t,res}$; dashed lines (·-): Mohr's circles above $\psi_{t,res}$; solid markers (•): points on the circles used for plane-fitting.

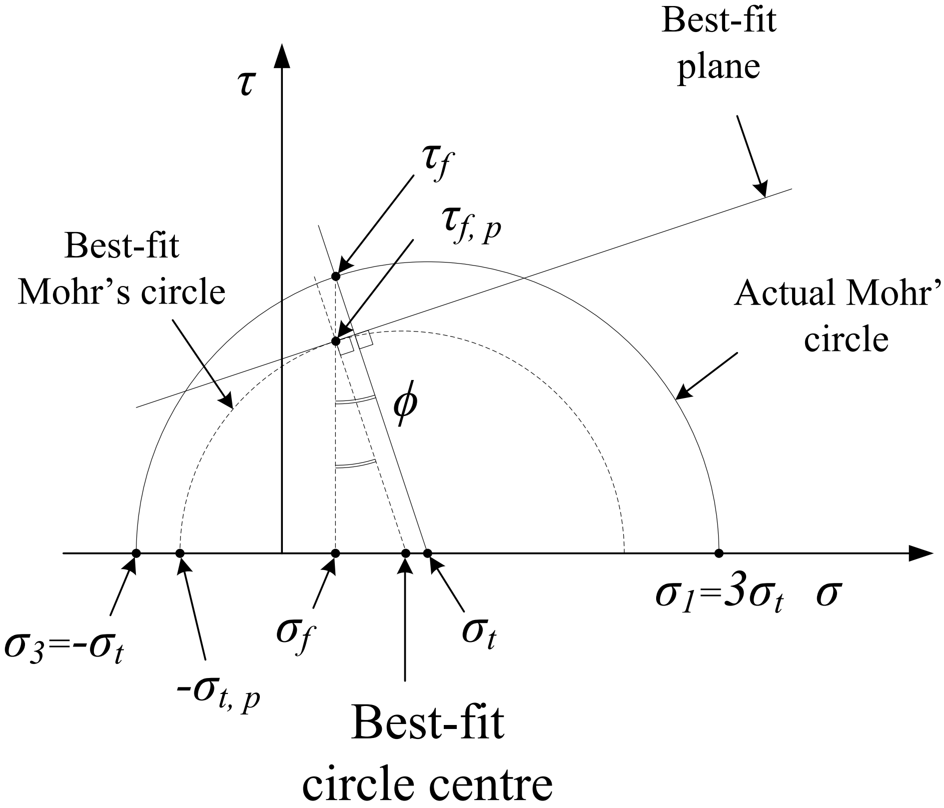


Figure 10: Geometrical relationships between predicted and measured strength values

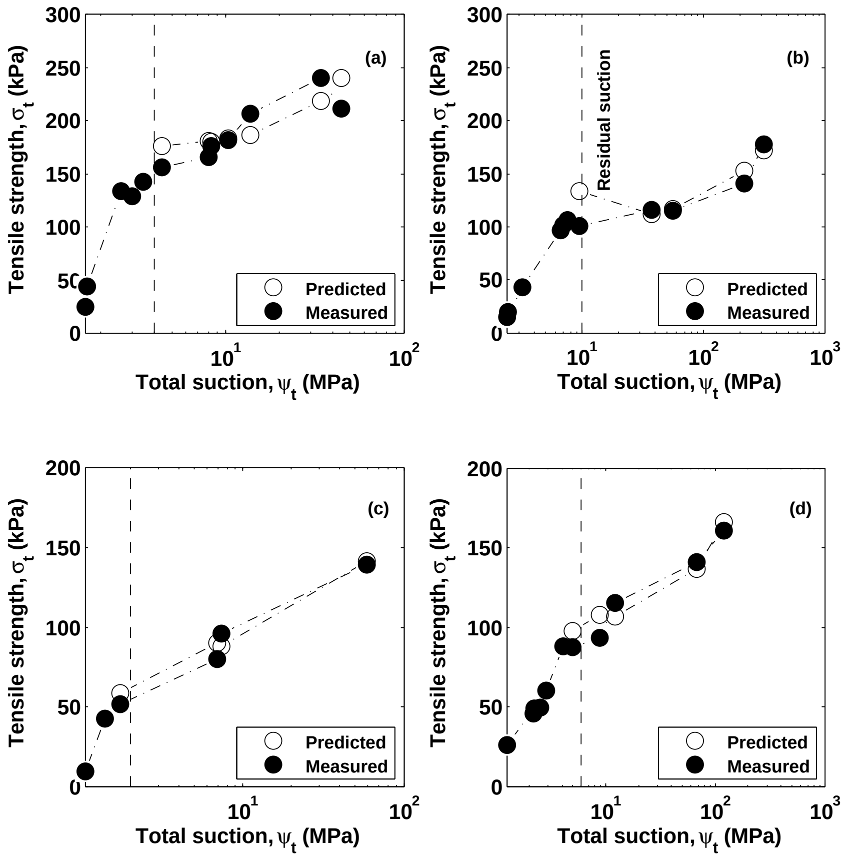


Figure 11: Measured and predicted ($\geq \psi_{t,res}$) tensile strengths for tested soil conditions: a) 4-5-1, untreated; b) 4-5-1, treated; c) 2-7-1, untreated; d) 2-7-1, treated.

## 5. Conclusions

This paper investigated the effect of $CaCl_2$ addition on the tensile strength of two compacted engineered soils equilibrated to a range of suction conditions. Contrary to literature results, the traditional decrease in tensile strength on flocculant addition was not found for a soil with a low clay content. Soil retention properties were used in combination with an EMC analysis to examine this behaviour. It was determined that $CaCl_2$ addition decreased the contribution of suction to strength ($\phi^b_{res}$) in both soils. However, material cohesion ($c_{res}$) for suctions $> \psi_{t,res}$ increased for Soil 2-7-1 but decreased for Soil 4-5-1, resulting in the observed changes in $\sigma_t$ as the soils dried. Changes in soil flocculation susceptibility therefore have a significant effect on resulting soil properties. Similarities between treated material tensile strength and detailed analyses of soil structural changes using SEM, XRCT and/or MIP are subjects for further investigation.

## 6. Acknowledgements

The first author was supported by a studentship awarded by the School of Engineering and Computing Sciences, Durham University whilst this research was undertaken and is now supported by ARC Linkage Grant LP110100251. The authors would like to thank Profs. Alessandro Tarantino and David Toll for their comments on this work.

## References


ASTM, 2010. ASTM D5298-10. Standard test method for measurement of soil potential (suction) using filter paper.

Barzegar, A., Murray, R., Churchman, G., Rengasamy, P., 1994a. The strength of remolded soils as affected by exchangeable cations and dispersible clay. Australian Journal of Soil Research 32 (2), 185–199.

Barzegar, A. R., Oades, J. M., Rengasamy, P., 1996. Soil structure degradation and mellowing of compacted soils by saline sodic solutions. Soil Science Society of America Journal 60 (2), 583–588.

Barzegar, A. R., Oades, J. M., Rengasamy, P., Giles, L., 1994b. Effect of sodicity and salinity on disaggregation and tensile strength of an alfisol under different cropping systems. Soil & Tillage Research 32 (4), 329–345.

Beckett, C. T. S., 2011. The role of material structure in compacted earthen building materials: Implications for design and construction. PhD Thesis, Durham University.

BSI, 1990. BS 1377:1990. Methods of testing for soils for civil engineering purposes.

Clayton, C. R. I., Matthews, M. C., Simons, N. E., 1995. Site Investigation. Oxford (UK); Cambridge, Mass. (USA): Blackwell Science.

Consoli, N., Da Silva Lopes Jr, L., Consoli, B. S., Festugato, L., 2014. Mohrcoulomb failure envelopes of lime-treated soils. Géotechnique 64 (2), 165–170.

Dao, V. N. T., Morris, P. H., Dux, P. F., 2008. On equations for the total suction and its matric and osmotic components. Cement and Concrete Research 38 (11), 1302–1305.

Deng, Y. F., Yue, X. B., Cui, Y.-J., Shao, G. H., Liu, S. Y., Zhang, D. W., 2014. Effect of pore water chemistry on the hydro-mechanical behaviour of Lianyungang soft marine clay. Applied Clay Science 95, 167–175.

Dexter, A., Kroesbergen, B., 1985. Methodology for determination of tensile strength of soil aggregates. Journal of Agricultural Engineering Research 31 (2), 139–147.

Dexter, A. R., Chan, K. Y., 1991. Soil mechanical properties as influenced by exchangeable cations. Journal of Soil Science 42 (2), 219–226.

Dontsova, K. M., Norton, L. D., 2002. Clay dispersion, infiltration, and erosion as influenced by exchangeable ca and mg. Soil Science 167 (3), 184–193.

Fredlund, D. G., Morgenstern, N. R., Widger, R. A., 1978. The shear strength of unsaturated soils. Canadian Geotechnical Journal 15 (3), 313–321.

Fredlund, D. G., Xing, A., 1994. Equations for the soil-water characteristic curve. Canadian Geotechnical Journal 31 (4), 521–532.

Fredlund, D. G., Xing, A., Fredlund, M. D., Barbour, S. L., 1996. The relationship of the unsaturated soil shear strength functions to the soil-water characteristic curve. Canadian Geotechnical Journal 32, 440–448.

Frydman, S., 1964. The applicability of the Brazilian (indirect tension) test to soils. Australian Journal of Applied Science 15, 335–343.

Grant, C. D., Dexter, A. R., Oades, J. M., 1992. Residual effects of additions of calcium compounds on soil structure and strength. Soil & Tillage Research 22 (3-4), 283–297.

Hall, M., Djerbib, Y., 2004. Rammed earth sample production: context, recommendations and consistency. Construction and Building Materials 18 (4), 281–286.

Hamblin, A. P., 1981. Filter paper method for routine measurement of field water potential. Journal of Hydrology 53 (3/4), 355–360.

Jaeger, J. C., Cook, N. G. W., Zimmerman, R. W., 2007. Fundamentals of rock mechanics. Blackwell Publishing.

Li, D., Wong, L. N. Y., 2013. The Brazilian disc test for rock mechanics applications: Review and new insights. Rock Mechanics and Rock Engineering 46, 269–287.

Lu, N., Wu, B., Tan, C. P., 2007. Tensile strength characteristics of unsaturated sands. Journal of Geotechnical and Geoenvironmental Engineering 133 (2), 144–154.

Rocco, C. G., Guinea, G. V., Planas, J., Elices, M., 1999. Size effect and boundary conditions in the Brazilian test: Experimental verification. Materials and Structures 32, 210–217.

Rycroft, D. W., Kyei-Baffour, N., Tanton, T., 2002. The effect of sodicity on the strength of a soil surface. Irrigation and Drainage 51 (4), 339–346.

Schubert, H., 1975. Tensile strength of agglomerates. Powder Technology 11, 107–119.

Smith, J. C., Augarde, C. E., 2013. Optimum water content tests for earthen construction materials. Construction Materials 167 (2), 114–123.

Smith, J. C., Augarde, C. E., September 1–3 2014. XRCT scanning of unsaturated soil: Microstructure at different scales? In: Geomechanics from Micro to Macro. University of Cambridge, pp. 1137–1142.

Song, Y.-S., Hwang, W.-K., Jung, S.-J., Kim, T.-H., 2012. A comparative study of suction stress between sand and silt under unsaturated conditions. Engineering Geology 124, 90–97.

Sou/Dakouré, M. Y., Mermoud, A., Yacouba, H., Boivin, P., 2013. Impacts of irrigation with industrial treated wastewater on soil properties. Geoderma 200–201, 31–39.

Stirling, R. A., Hughes, P., Davie, C. T., Glendinning, S., 2015. Tensile behaviour of unsaturated compacted clay soils — A direct assessment method. Applied Clay Science online.

Williams, D., Jones, H., 2005. Tailings storage facilities. In: Wills, B. A. (Ed.), Advances in Gold Ore Processing. Vol. 15 of Developments in Mineral Processing. Elsevier, Amsterdam, The Netherlands, Ch. 30, pp. 729–752.

## Figure captions

1. Particle grading curves for Soils 4-5-1 and 2-7-1 (untreated)
2. Failure of Brazilian test samples indicating non-vertical and vertical failure cracks: a) 50 mm diameter 25 mm high; b) 100 mm diameter 50 mm high. Outlines and shading added for clarity.
3. Treated and untreated SWRCs for soil 4-5-1. White markers show drying suction conditions for treated and untreated Brazilian test specimens.
4. Treated and untreated SWRCs for soil 2-7-1. White markers show drying suction conditions for treated and untreated Brazilian test specimens.
5. Tensile strength against degree of saturation for treated and untreated Soil 4-5-1 specimens
6. Tensile strength against degree of saturation for treated and untreated Soil 2-7-1 specimens
7. Comparison of treated Soil 4-5-1 and 2-7-1 results, with descriptive linear trends.
8. Example Brazilian test EMC failure surface construction
9. EMC failure surface for untreated Soil 4-5-1 above $\psi_{t,res}$. Solid lines (–): Mohr's circles below $\psi_{t,res}$; dashed lines (·-): Mohr's circles above $\psi_{t,res}$; solid markers (•): points on the circles used for plane-fitting.
10. Geometrical relationships between predicted and measured strength values
11. Measured and predicted ($\geq \psi_{t,res}$) tensile strengths for tested soil conditions: a) 4-5-1, untreated; b) 4-5-1, treated; c) 2-7-1, untreated; d) 2-7-1, treated.

## Table captions

1. Soil constituents, OWC and $\rho_{d_{max}}$
2. Fitting parameters used with Eqn 4
3. Fitted EMC failure surface parameter values